Performance vs. Survivability: Evaluation of a Range of Control Strategies in a 1MW Oscillating Wave Surge Converter (OWSC)

Laporte Weywada P., Scriven J., Matysiak A., König R., May P.J.C., Roeber V., Kalisch H.

Abstract—**The MegaRoller project, funded under the European Union's Horizon 2020 research and innovation programme, aims to develop and demonstrate a novel Power Take-Off (PTO) solution for Wave Energy Converters (WECs). As part of the project, a wave-by-wave prediction software was developed, with a neural network prediction algorithm at its core. In this paper, the impact of the control strategy on key metrics is considered, focusing on assessing the potential of such wave-by-wave prediction software in improving the power performance and survivability of the system. In particular, two applications are considered: in a first step, a wave-by-wave damping adjustment control strategy, aiming at maximising the power capture, is compared to a baseline control strategy. When considering the additional complexity of the control system, the limited gains in power production suggest that, for the MegaRoller device, wave-by-wave damping control may not be beneficial enough. In a second step, methods for utilising the twin drive-trains of the MegaRoller device to counteract undesirable torque loads on the bearings in cases of oblique waves are investigated, comparing a baseline case to the application of an asymmetrical force in the PTO cylinders, adjusted either on a sea state by sea state, or a wave-by-wave basis. Such approach is shown to significantly improve the system's survivability, reducing torque loads on the bearings. The impact of error on the wave-by-wave prediction is also shown to have a minimal impact on the metrics considered, providing confidence in the suitability of the prediction tool developed for the proposed purpose.**

Keywords—**Control strategy, MegaRoller, Power Take-Off (PTO), numerical modelling, Oscillating Wave Surge Converter (OWSC), wave-by-wave control, wave energy.**

I. Introduction

EFFICIENCY and reliability are two key challenges in the design for Power Take-Offs (PTOs) for wave energy converters (WECs), because waves generate slow and irregular oscillations, which require a PTO to generate large alternating reacting forces in order to extract power. The MegaRoller project aims to tackle these challenges with the design, construction and validation of a generic high performance, reliable and cost-efficient 1MW PTO that can be integrated into Oscillating Wave Surge Converter (OWSC) designs.

The development of the PTO for a 1MW OWSC device is based on multiple software and hardware innovations. One of the key software innovations of the MegaRoller project focuses on the development of a wave-by-wave control strategy for the WEC system, aiming to optimise the power capture of the system.

For these purposes, the MegaRoller consortium is developing a wave-by-wave prediction software with a neural-network prediction algorithm at its core. For design and network training purposes, this data is provided either from hindcasts, buoy records or dedicated runs using a phase-resolving nearshore model. In an operational setting, the measurements will most likely be provided by a dedicated survey buoy moored in proximity to the WEC. The measured time series is then fed into an echo state network (ESN) in order to compute a prediction of the surface elevation associated to the next few incoming waves. Based on the output from the prediction software, the MegaRoller PTO settings will be optimised in terms of damping characteristics at each of the two drive-trains on a wave-by-wave basis. It should be noted that this innovation could have numerous other marine

ID number 2008, track GPC.

This project has received funding from the European Union's Horizon 2020 research and innovation programme under grant agreement No 763959.

J. Scriven and P. Laporte Weywada work at K2 Management Lda, Rua do Montepio Geral, N.4-A, 1500-465 Lisboa, Portugal (respective e-mails: jos@k2management.com and plw@k2management.com).

A. Matysiak and R. König work at Leibniz Institute for Neurobiology, Brenneckestraße 6, Magdeburg 39118, Germany (respective e-mails: artur.matysiak@lin-magdeburg.de, rkoenig@lin-magdeburg.de).

P.J.C. May is affiliated with the Department of Psychology, Lancaster University, Lancaster, LA1 4YF, United Kingdom, and with the Leibniz Institute for Neurobiology (address above) (e-mail: p.may1@lancaster.ac.uk).

V. Roeber works at Université de Pau et des Pays de l'Adour, Anglet campus, IPRA, EA4581, 64600, Anglet, France (e-mail: volker.roeber@univ-pau.fr).

H. Kalisch works at the Department of Mathematics, University of Bergen., PO Box 7800, 5020 Bergen, Norway (e-mail Henrik.kalisch@uib.no).

applications, such as predicting when dynamically positioned ships may encounter a larger wave, or when best to launch a freefall lifeboat.

In this work, the development of the wave-by-wave prediction model and control strategy will be described. The paper will then focus on the assessment of the impact of the control strategy on key power performance and survivability metrics, using a distributed, fully coupled, nonlinear WEC loads model of the 1MW OWSC system. In particular, methods for utilising the twin drive-trains of the MegaRoller device to counter-act undesirable torque loads on the bearings will be investigated and compared for different wave cases and control strategies, from a baseline case to the application of a wave-by-wave varying counterforce in one of the PTO cylinders, in cases of waves approaching from an oblique heading. While contributing to the efficient capture of energy from the wave field, such an approach also aims to increase the survivability of the system by maintaining a fair distribution of the loads, and reducing torque loads on the bearings and the WEC prime mover. The impact of error on the wave-by-wave prediction will also be assessed.

The loads model will be developed in the WEC-Sim software, customised for use in performance, load and structural assessments, aiming to assess the influence of the distributed loading contributions over the WEC prime mover, accounting for the coupled nature of interaction(s) between the flap and the PTO load sources.

This paper is organised in five main sections. Following this introduction (Section I), the MegaRoller system is described in Section II, focusing on the wave prediction system developed and the control strategies envisaged for the WEC. The methodology for the study is then presented in Section III, describing the load analysis model of the MegaRoller WEC developed in the WEC-Sim tool, as well as the scenarios and key metrics considered. The results of the investigations conducted, looking at the performance and survivability metrics of interest, are then presented in Section IV. Finally, the recommended next steps, in particular regarding the future development of a control strategy, are detailed in Section V.

II. MegaRoller System

A. *Technical description of the MegaRoller WEC*

The MegaRoller WEC was described, at a high level, in [1]. Essentially, the MegaRoller WEC can be described as an OWSC with an innovative, modular PTO solution, where hydraulic piston pumps have an interface with the panel via a twin drive-train located at each end of the WEC's prime mover (flap). The pistons pump hydraulic fluid inside a closed circuit, which is enclosed inside a hermetic structure and thus not exposed to the marine environment. The high-pressure fluids are fed into hydraulic motors that drive a generator. Finally, the electrical output from the generator is fed to the electric grid via a subsea cable (see Fig. 1).

The device operates in nearshore regions at depths of between 8 and 20 metres. It is anchored to the seabed and, depending on mean depth and tidal range, it is mostly or fully submerged during operation. A series of devices can be deployed in an array to create a WEC farm. Since the WEC is constructed as a modular individual unit, there is no technical upper limit to the number of devices that can be used in an array.

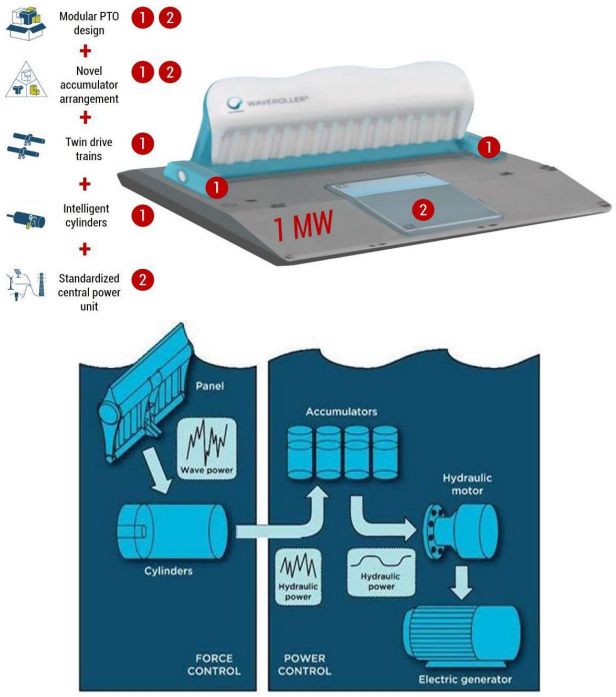

Fig. 1. 1MW OWSC device (top) and OWSC conversion process (bottom)

The target geometric and mass properties of the MegaRoller WEC prime mover (the flap) are summarised in TABLE I. The main dimensions of the WEC are illustrated in Fig. 2. Given the early stage of the design, the overall properties are generic and subject to further refinement.

TABLE I
KEY GEOMETRIC AND MASS PROPERTIES OF THE MEGAROLLER WEC PRIME MOVER (FLAP)

Property	Unit	Value
Volume	m^3	750
Mass	kg	250,000
Moment of inertia I_{yy}	kgm^2	5,000,000
Location of the centre of gravity[a]	m	5.3
Location of the centre of buoyancy[a]	m	7.5
Location of the bearings[a]	m	3
Location of the PTO[a]	m	5

[a]Locations (in metres) refer to vertical positions in the water column measured from the seabed.

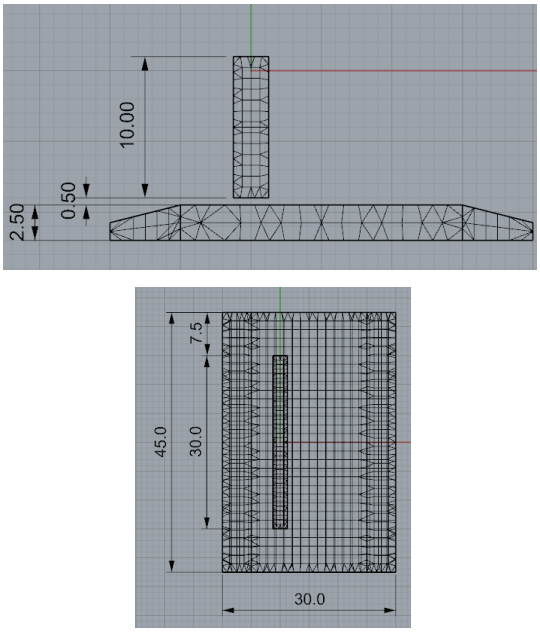

Fig. 2. MegaRoller WEC dimensions (in m) – side and top views. The red and green axis correspond to the x and z axis of the coordinate system, respectively (origin at water level)

B. *Wave prediction system*

For the efficient operation of the control algorithm, accurate prediction of the incoming wave field is key. Wave forecasting methods can be classified into two broad categories, according to whether the model is based on underlying physical principles, or on data analysis. The physics-based approach relies on numerical simulation of partial differential equations, which yield spectral information about the expected sea states. One example is the SWAN wave-forecasting package for use in coastal seas [2].

The second approach relies either on statistical techniques such as regression analysis or on neural networks ([3] to [5]). Since the underlying physics is not taken into account, accurate prediction using the data-based approach is naturally restricted to a more limited time horizon of about six hours [6]. However, for applications in wave energy, short-term forecasts of about 15 to 30 minutes are sufficient if the control algorithm is adjusted only once for each sea state. For a wave-by-wave forecast, a time horizon of about two-three wave periods should be sufficient. For example, it was shown in [7] that at most a 30-second forecast horizon would be required for heave-type devices of cylindrical or spherical shape. Given the recent surge in deep learning techniques, the neural-network method has been a popular device for short-term wave forecasting (see for example [8]).

In the framework of ESNs, the time series is fed as input to a neural network with fixed structure and weights, and the units of the network are connected to an output unit. During training, only the output weights are changed through linear regression, which makes echo state networks computationally efficient. For prediction, the input is replaced by feedback from the output unit. In most applications, the reservoir is a random neural network, and there has been little evidence that the structure of the reservoir has any significant effect on predictive performance. However, preliminary experimentation showed that the effect of structure may be specific to the data and task at hand.

In the present work, both physics-based and data-based approaches were tested. For the representation of sea states, predictions from a SWAN hindcast were used. In addition, wave-by-wave control strategies which require phase-resolving wave data were also tested. For this purpose, simulations of a Boussinesq-type model [9] and predictions using ESN-types of artificial neural networks were employed. The Boussinesq model generally performed better than the ESN, and it was used in connection with the load characterisation of the wave energy device. However, as mentioned above, an in-depth study of the exact structure of the network may lead to improved performance.

C. *Control strategies for power production*

The baseline control strategy for the MegaRoller device assumes that the force F_{PTO} applied to the prime mover by the PTO is proportional to the linear velocity of the PTO stroke (i.e. a damping force):

$$F_{PTO,total} = c(H_s, T_p, \theta) \cdot v \tag{1}$$

where c is the damping constant and v is the PTO stroke velocity, converted from the angular motion of the flap.

In the baseline control strategy, c is optimised for each sea state, characterised by a significant wave height (H_s), peak period (T_p) and mean direction (θ), in order to maximise the mean power extracted. The optimisation was conducted using a numerical study, whereby several damping coefficients (c) were trialled in order to identify the value which resulted in the maximum absorbed power. An equal force is applied to both drive-trains:

$$F_{PTO,1} = F_{PTO,2} = \frac{F_{PTO,total}}{2} \tag{2}$$

The force in each PTO is additionally limited by a force cap (F_{max}), whereby:

$$F_{PTOcap,i} = min\begin{cases} F_{max} \\ F_{PTO,i} \end{cases} \tag{3}$$

The baseline strategy does not require any advance knowledge of the approaching waves but rather an estimation of the current sea state parameters (e.g. H_s). These parameters vary relatively slowly (e.g. every 30 minutes).

In an alternative approach, the wave prediction system introduced in Section II.B can be used to vary the applied PTO damping on a wave-by-wave basis. Instead of optimising the damping constant (c) for each sea state, it can be optimised for each individual wave height and period using regular wave simulations.

$$F_{PTO,total} = c(H,T,\theta) \cdot v \quad (4)$$

It is hypothesised that this approach would allow for more optimised control of the MegaRoller device, increasing power performance.

D. Control strategies for load reduction

A second potential application of wave-by-wave control is to reduce loads on key components, increasing the survivability of the device and/or enabling a reduction in CAPEX. In particular, the MegaRoller WEC does not have a degree of freedom in yaw. In cases of waves approaching from an oblique heading, a hydrodynamic torque load ($M_{z,hydro}$) is therefore generated about the bearings which connect the prime mover to the foundation.

To counter-act the hydrodynamic torque load generated and to reduce the total torque on the bearings, a more advanced control algorithm can be defined, in which the total PTO force is split unequally between the two drive-trains using a constant factor a_1:

$$\begin{aligned} F_{PTO,1} &= a_1 \cdot F_{PTO,total} \\ F_{PTO,2} &= (1 - a_1) \cdot F_{PTO,total} \end{aligned} \quad (5)$$

The total applied force remains the same and so, in the WEC-Sim model, the power extraction is unaffected. It is noted that the WEC-Sim model could, in future work, be further developed so that the potential consequences on the resulting operating states can be evaluated.

Two different approaches to this strategy were investigated.

In the first approach (referred to as 'constant offset'), the factor a_1 is varied on per-sea-state , similar to the damping coefficient in (1), i.e. a_1 is a function of H_s, T_p and θ. Similar to the baseline strategy (see Section II.C), this approach does therefore not require any advance knowledge of the incident wave, but rather an estimation of the current sea state parameters.

In a second approach (referred to as 'wave-by-wave'), the wave prediction system introduced in Section II.B is used to predict the hydrodynamic torque load on the bearing. As an initial approximation, and in the case of irregular waves, the hydrodynamic torque was assumed to be linearly proportional to the predicted surface elevation, with different scaling factors derived for each wave height, period and direction using regular wave simulations:

$$M_{z,hydro} = b(H,T,\theta) \cdot z \quad (6)$$

where b is a linear scaling factor and z is the predicted surface elevation. Future work could seek to refine this estimation, using more advanced hydrodynamic models.

The PTO forces are then varied on a wave-by-wave basis in attempt to 'cancel out' the bearing torque in real-time:

$$l.F_{PTO,1} - l.F_{PTO,2} + M_{z,hydro} = 0 \quad (7)$$

where l is the lever arm of each PTO relative to the bearings. In this case, the bearings are assumed to be in the centre of the prime mover.

Essentially, the a_1 factor used to minimise the total bearing torque on a wave-by-wave basis can therefore be estimated by combining equations (5) and (7):

$$a_1 = \left(l.F_{PTO,total} - M_{z,hydro}\right)/2lF_{PTO,total} \quad (8)$$

For both approaches, the force cap is also applied, unchanged from the baseline strategy (see (3)).

III. METHODOLOGY

A. MegaRoller WEC-Sim model

WEC-Sim (Wave Energy Converter SIMulator) [10] is an open-source WEC simulation tool, developed in MATLAB/Simulink using the multi-body dynamics solver SimMechanics. The WEC-Sim project is funded by the U.S. Department of Energy's Wind and Water Power Technologies Office, and the code development effort is a collaboration between the National Renewable Energy Laboratory (NREL) and Sandia National Laboratories (SNL).

The WEC-Sim model of the MegaRoller WEC developed in [1] was used as a starting point for this study. The model, shown in Fig. 3, consists of the prime mover, which is connected to the fixed base and reference frame, using a rotational degree-of-freedom to represent the bearing. Each of the two PTO drive-trains are modelled using a linear actuator, connected on one end to the prime mover using a level arm, effectively transforming linear to a rotational load, and a fixed base connection using a rotational joint located at the opposite side of the actuator.

The PTO control logic was adapted to implement the new control strategies, specifically to allow the two PTO forces to be set from a central control module. This control module implements the following high-level process:

1. Use the instantaneous rotational speed and knowledge of the sea state to calculate the target damping coefficient and target total PTO force according to (1).

2. Use the predicted wave elevation to estimate the hydrodynamic torque on the bearing according to (6).

3. Calculate the two PTO force to minimise the total bearing torque according to (7).

4. Command each PTO to implement its own target force, after applying the force cap (2) if applicable.

As an initial approximation, it was assumed that the wave prediction system introduced in Section II.B allows exact prediction of the surface elevation, with sufficient lead-time in order to adjust the controller as required. The effect of possible inaccuracies in the wave prediction is then investigated further in Section IV.D.

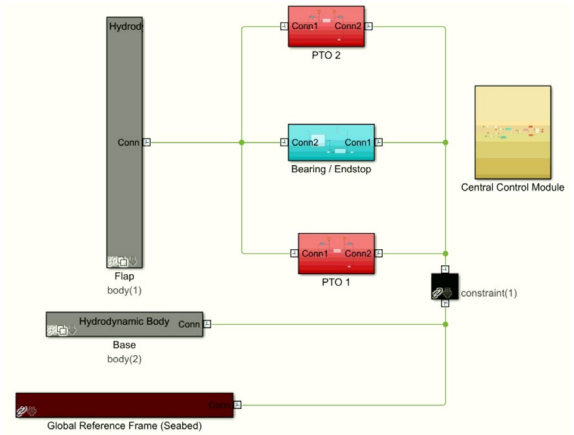

Fig. 3. WEC-Sim model. The added 'central control module' is shown in yellow.

B. *Scenarios and load cases*

This study aimed at investigating the potential benefits of the wave-by-wave prediction tool in the performance and survivability of the system, defined as its ability to withstand extreme loading events and high fatigue cyclic loading. In particular, for a PTO and/or WEC to demonstrate survivability it must withstand very high-duty = cyclic loading. This study therefore focused on fatigue loading and considered normal operating conditions. Extreme loads are likely to be driven by more extreme sea states and/or fault scenarios, which were outside the scope of this study.

In a first step, the study investigated the impact of the wave-by-wave control strategy in regular waves. An illustrative regular wave with height (H) of 1m and period (T) of 12s was considered, assumed to approach the MegaRoller device with a mean heading (θ) of 15°.

The study then looked at irregular waves, using as reference the climate conditions at the Peniche site (Portugal). A series of sea states, characterised by H_s, T_p and θ, were down selected for analysis, and are outlined in TABLE II.

Percentage occurrences of each sea state were derived from a 10-year SWAN wave dataset (covering the period between January 1997 and December 2006). The occurrences for each direction are summarised in the Appendix, and Fig. 4 presents the omni-directional occurrence matrix, which was used for power production assessments. The selected sea states cover 89% of all occurrences recorded at Peniche.

All irregular sea states were simulated assuming a Pierson-Moskowitz spectra with peak amplification factor (γ) equal to 1. TABLE III lists some other key simulation parameters.

TABLE II
DESIGN LOAD CASE AND SELECTED SEA STATES

Property	Unit	Value
Operating Condition	-	Normal, Power Production
Water depth	m	12.0
Significant wave height	m	0.75 : 0.5 : 4.25
Peak period	s	7 : 2 : 15
Mean direction	°	0 : 5 : 30

H_s [m] / T_p [s]	7	9	11	13	15
0.75	2.3%	6.3%	3.1%	0.8%	0.2%
1.25	4.2%	8.5%	9.1%	3.7%	0.9%
1.75	3.1%	4.9%	10.5%	6.1%	1.5%
2.25	0.6%	2.2%	5.3%	6.3%	1.8%
2.75	0.0%	0.9%	2.1%	4.5%	1.9%
3.25	0.0%	0.3%	0.8%	2.4%	1.9%
3.75	0.0%	0.1%	0.3%	0.9%	1.4%
4.25	0.0%	0.0%	0.1%	0.3%	0.6%

Fig. 4. Omni-directional percentage occurrence for selected sea states, scaled to 100% total.

TABLE III
WEC-SIM SIMULATION PARAMETERS

Property	Unit	Value
Simulation length	s	3800
Ramp-up time	s	200
Time step	s	0.01
Hydrostatic force calculation	-	Linear
Wave spreading	-	None

C. *Key metrics*

The power performance of the MegaRoller device was assessed using the mean power for a given sea state, output by WEC-Sim. It should be noted that this is essentially the mechanical power at the PTO interface and does not include any hydraulic or electrical losses. In addition, wave direction was not considered for these studies and all waves were assumed to approach the MegaRoller device head-on.

Values for each sea state were combined into a single Mean Estimated Annual Power (MAEP) estimate as outlined below:

$$MAEP = t \cdot \sum_{i=1}^{i=n} p_i \cdot \overline{P_i} \tag{9}$$

where p_i is the probability of occurrence of each sea state, $\overline{P_i}$ is the mean power, summed for both PTOs, and t is the annual operating time (100% availability was assumed in this study).

Regarding survivability, two key load metrics were used to assess the impact of the different control strategies on the bearing torque loads. As the investigations conducted focused on normal sea states and normal operating conditions, these metrics focused on fatigue loading.

The first load metric used was the Root-Mean-Square (RMS) of the bearing torque. This simple metric gives an initial approximation of the magnitude of the torque loading, deemed acceptable in operational conditions. It is noted that, in case of extreme events (not considered here), such approach would unlikely be conservative.

The second load metric was the Damage Equivalent Load (DEL), which gives a more accurate measure of the fatigue loading by taking account of the material Wohler exponent (m). The DEL is given by:

$$DEL = \left(\sum_{i=1}^{i=k} \frac{n_i \cdot {L_i}^m}{N_{eq}} \right)^{1/m} \quad (10)$$

where n is the number of load cycles at a specific load range (L) N_{eq} is a reference number of cycles (1E+07 was used in this study) and m is the Wohler exponent (m =3 was used in this study, assuming a welded steel material).

IV. Results

A. Power production

To investigate the effects of wave-by-wave damping control on power production, following the approach described in Section II.C, the same sea states were analysed using the baseline (1) and wave-by-wave (4) damping control approaches. Fig. 5 shows the percentage increase in mean power for each sea state when switching to a wave-by-wave control strategy compared to the baseline approach (1). Percentage increases are largest in smaller significant wave heights. This is likely due to the force cap, which 'saturates' the controller in larger sea states and removes any potential benefit of the more optimised damping.

As defined in (9), MAEP was used to compare the overall power performance. Table IV shows that the overall increase in power is small, with an increase of 1.5% due to wave-by-wave control. When considering the additional complexity of the control system, this suggests that, for the MegaRoller device, wave-by-wave control may not be beneficial in terms of power production.

It is hypothesised that the limited benefit of the wave-by-wave damping control strategy for the MegaRoller WEC may be due to the device's characteristics, specifically the fact that the device is not designed to resonate with the waves like other devices (e.g. point absorbers). In addition, the WEC geometry may not be optimised for the control strategy considered (see also [11]). It is also hypothesised that the force cap may also be a limiting factor in the performance gains obtained by this control approach.

Nonetheless, more complex control strategies (e.g. introducing a potentially adjustable 'stiffness' or 'mass' term into (4), see e.g. [12]) may increase the power capture. Future work could seek to investigate this further, especially to compare any potential performance gains against the required increase in complexity of the PTO drive-trains (e.g. to enable the PTO to input power).

Table IV
MAEP using the baseline and wave-by-wave control approaches

Property	MAEP [MWh]	Capacity factor [%]
Baseline	3392	38.7%
Wave-by-wave	3442	39.2%

H_s [m] / T_p [s]	7	9	11	13	15
0.75	0.5%	1.3%	3.5%	4.2%	3.6%
1.25	0.5%	1.3%	3.1%	3.7%	3.2%
1.75	0.5%	1.0%	2.4%	2.9%	2.6%
2.25	0.3%	0.7%	1.5%	2.1%	1.9%
2.75	0.2%	0.4%	0.9%	1.4%	1.2%
3.25	0.1%	0.2%	0.6%	0.9%	0.6%
3.75	0.1%	0.1%	0.3%	0.5%	0.3%
4.25	0.0%	0.0%	0.1%	0.3%	0.1%

Fig. 5. Percentage increase in mean power when using a wave-by-wave controller compared to the baseline controller.

B. Initial bearing load tests – regular waves

When investigating the potential benefits of wave-by-wave control in terms of load reduction on the bearings, following the approach described in Section II.D, the control strategy was first tested using a regular wave case. In such wave conditions, the hydrodynamic torque can be determined exactly (i.e. by running the simulation in advance with the baseline controller). As shown in Fig. 6, the wave-by-wave controller is therefore able to significantly reduce the total torque on the bearing. In the case considered ($H = 1.00m, T = 12s, \theta = 15°$), the RMS value was reduced by over 80%.

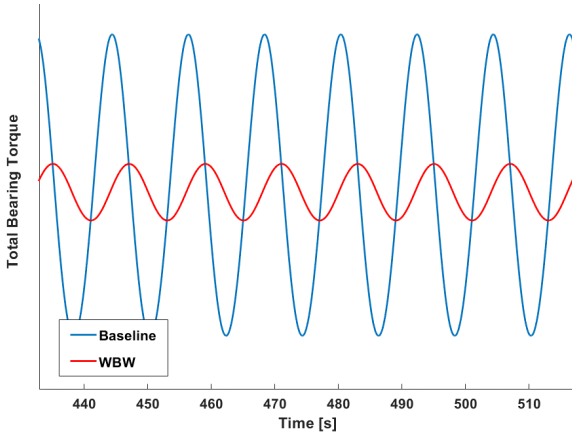

Fig. 6. Total bearing torque when using the baseline (in blue) and wave-by-wave (in red) controllers. H= $1.00m, T = 12s, \theta = 15°$

C. Bearing loads - Irregular sea states

After demonstrating the benefits of the wave-by-wave control strategy on the bearing torque in regular waves, the study was extended in a next step to more realistic, irregular sea states.

The main difference when compared with regular waves is the complexity introduced by irregular waves in the prediction of the hydrodynamic torque on the bearing. Fig. 7 compares the estimated torque when using the simplified approach outlined in (6), where the torque is assumed to be proportional to the surface elevation, with the actual time series (run as a separate simulation using a baseline controller setting), for an illustrative irregular wave case ($H_s = 1.75m, T_p = 11s, \theta = 15°$). Whilst the predicted time-series can generally be considered to be adequate for this initial, proof-of-concept study, it can probably be improved in future development works, notably in smaller, shorter period waves, e.g. by using more advanced hydrodynamic models and tools such as machine learning.

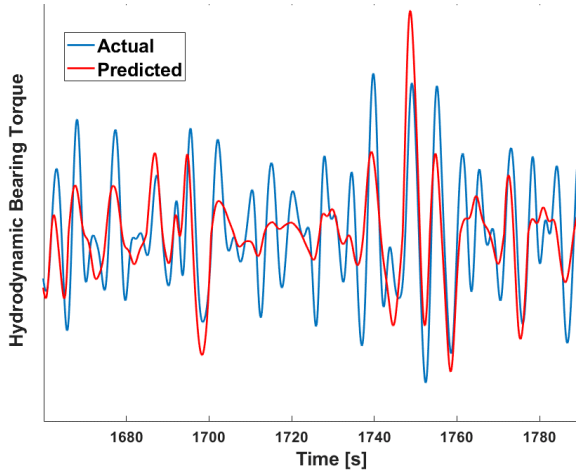

Fig. 7. Actual vs predicted hydrodynamic bearing torque $H_s = 1.75m, T_p = 11s, \theta = 15°$

Fig. 8 shows the resulting total torque on the bearing, comparing the baseline controller with the 'wave-by-wave' and 'constant offset' approaches. As expected, both methods are shown to reduce the total torque on the bearings. However, this reduction is relatively small for the 'constant offset' approach (in blue) – with an approximately 4% decrease in RMS of bearing torque. The wave-by-wave approach (in red) shows better results, with, quantitively, peak values visibly reduced, and a c.24% decrease in RMS of bearing torque compared to the baseline approach.

As a final step, all the sea states outlined in Table II were considered, using the three control strategies. Fig. 9 and TABLE V summarise the resulting reductions in RMS and DEL of bearing torque compared with the baseline case (where both PTO forces are equal).

Overall percentage reductions in the order of 20-30% were observed in both RMS and DEL metrics for individual sea states when using the 'wave-by-wave' approach. The improvement is most significant in the region of 0.75-2.25m H_s. When weighted and combined into a single value, the DEL was reduced by 17.2% compared with the baseline case, where the 'constant offset' approach was only achieving a 3.8% reduction.

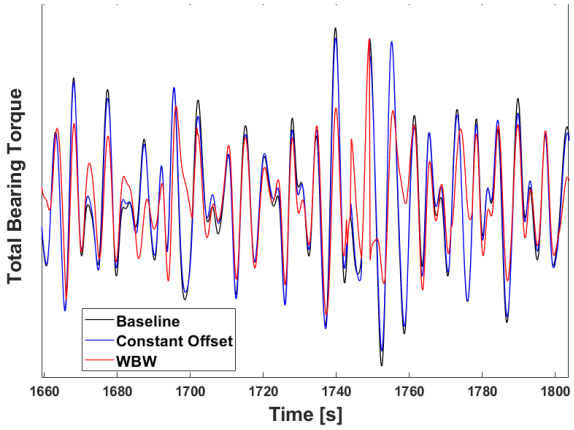

Fig. 8. Comparison of total bearing torque using three control strategies: baseline (in black), 'constant offset' (in blue) and wave-by-wave (in red). $H_s = 1.75m, T_p = 11s, \theta = 15°$

The wave-by-wave control strategy appears therefore clearly more effective in reducing the torque than the 'constant offset' approach. This shows the potential benefits of this control strategy, especially when considering the opportunities to further refine e.g. the hydrodynamic torque predictions.

H_s [m] / T_p [s]	7	9	11	13	15
0.75	27.3%	28.3%	26.0%	23.3%	20.1%
1.25	27.5%	28.3%	24.4%	22.9%	20.1%
1.75	20.7%	20.8%	19.8%	20.0%	18.4%
2.25	13.8%	14.2%	13.6%	15.4%	15.6%
2.75	9.1%	10.6%	9.0%	10.7%	11.1%
3.25	6.5%	7.1%	6.8%	6.7%	6.2%
3.75	4.2%	5.9%	5.2%	4.3%	4.5%
4.25	3.3%	4.6%	3.8%	2.7%	2.3%

Fig. 9. Percentage reduction in bearing torque DEL for irregular sea states approaching from a 15° heading when using a wave-by-wave control strategy.

TABLE V
PERCENTAGE REDUCTION IN WEIGHTED BEARING TORQUE USING DIFFERENT CONTROL STRATEGIES

Property	RMS	DEL
Baseline	-	-
Constant Offset	4.9%	3.8%
Wave-by-wave	23.5%	17.2%

It can be seen, e.g. in Fig. 9, that the percentage reduction tends to decrease as significant wave height increases. This is likely to be due to the PTO force cap (see (2)): As the total PTO force increases, the force cap limits the ability of the controller to react to the hydrodynamic torque. The only way of further reducing the total torque would therefore be to move away from the optimum PTO damping, such that both the total PTO force and the distribution between PTOs are varied. Such trade-off between power and loads could be studied further as part of any future work.

D. Influence of error in the wave prediction

The results presented in Section IV.C assume that the surface elevation can be predicted exactly. As outlined in

Section II.B, in practice some errors in the wave parameters predicted should be expected.

To investigate the potential effects of this error, the simulations were re-run with a random error in the prediction of each individual wave height and period, before calculation of the hydrodynamic bearing torque. The magnitude of each error was selected according to error histograms provided by the Leibniz Institute for a selection of different sea states (see Section II.B).

Three random errors were simulated for each sea state, each using the same surface elevation but introducing different random errors. Fig. 10 shows the resulting total bearing torque for an example sea state, in the baseline case (dashed), in the 'wave-by-wave' case with no error (black), and in the 'wave-by-wave' case with different errors (red, yellow and green). Fig. 11 shows the results for a mean wave direction of 15°, whilst Fig. 12 shows the weighted results for all wave directions.

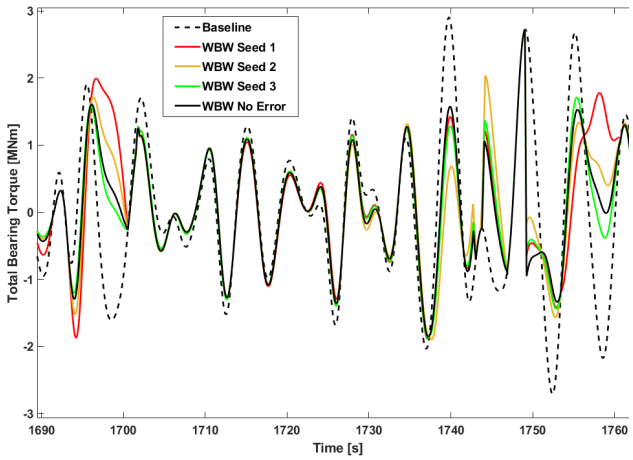

Fig. 10. Comparison of total bearing torque with and without error in the assumed wave elevation. $H_s = 1.75m, T_p = 11s, \theta = 15°$

Generally, differences introduced due to errors in the surface elevation prediction are small (<5%). This suggests that the wave prediction system's accuracy is adequate for this application. However, this should be re-visited if the hydrodynamic models were further improved, as this in turn may require a more accurate surface elevation prediction.

H_s [m] / T_p [s]	7	9	11	13	15
0.75	0.4%	0.5%	0.7%	1.4%	0.4%
1.25	0.0%	0.2%	0.5%	1.8%	1.9%
1.75	0.1%	0.5%	0.2%	1.9%	0.8%
2.25	0.1%	0.2%	0.3%	0.3%	3.5%
2.75	0.4%	0.2%	0.2%	0.5%	1.8%
3.25	0.3%	0.4%	0.2%	0.4%	1.1%
3.75	0.3%	0.3%	0.3%	0.3%	2.2%
4.25	0.1%	0.2%	0.2%	0.1%	1.4%

Fig. 11. Percentage difference (maximum – minimum) in RMS bearing torque between 3x random seeds for irregular sea states approaching from a 15° heading.

H_s [m] / T_p [s]	7	9	11	13	15
0.75	0.5%	0.8%	2.3%	2.6%	3.2%
1.25	0.4%	0.7%	1.0%	1.8%	4.0%
1.75	0.3%	0.5%	1.4%	2.3%	4.5%
2.25	0.3%	0.5%	0.9%	1.5%	3.5%
2.75	0.5%	0.4%	1.0%	1.2%	1.8%
3.25	0.4%	0.4%	0.6%	0.7%	2.7%
3.75	0.3%	0.3%	0.4%	1.2%	2.2%
4.25	0.1%	0.2%	0.4%	0.7%	1.8%

Fig. 12. Percentage difference (maximum – minimum) in RMS bearing torque between 3x random seeds for irregular sea states, all directions (weighted).

V. Conclusion

In this paper, the impact of the control strategy on key power performance and survivability metrics was considered, aiming in particular at assessing the potential benefits of a wave-by-wave prediction software for the power performance and survivability optimisation of the system.

In terms of power production, in the baseline control strategy PTO damping is only varied on a 'per sea state' basis. A wave-by-wave control strategy was defined in which the damping was updated for each individual wave, with the aim of increasing the total power absorbed.

The wave-by-wave approach was found to result in only a small increase (<2%) in MAEP. Overall, the results suggest that adjusting the PTO damping settings on a wave-by-wave basis is not likely to be beneficial when considering only power production. This is possibly due to the characteristics of the MegaRoller WEC, which is not designed to resonate with the approaching waves.

In terms of survivability, the study investigated the application of the wave-by-wave prediction tool to adjust, on a wave-by-wave basis, the PTO force split between the two cylinders of the MegaRoller twin drive-train. The study focused in particular on torque loads on the bearings. In the absence of a degree of freedom in yaw, waves approaching from an oblique heading typically generate a hydrodynamic torque load about the bearings that connect the prime mover to the foundation.

A control strategy was therefore defined where the hydrodynamic torque load generated is counteracted by an unequal split of the PTO force between the two drive-trains, to reduce the total torque on the bearings.

Overall, it was found that, while not affecting the capture of energy from the wave field, such asymmetrical PTO force split adjusted on wave-by-wave basis can significantly contribute to the survivability of the system when applied on a wave-by-wave basis (reducing the DEL bearing torque by more than 17% compared to the baseline strategy), and may represent therefore a potentially more suitable application of the wave-by-wave prediction tool. Error in the wave-by-wave prediction was found to have a minimal impact, with differences of less than 5% in RMS bearing torque.

A number of key next steps and future works were identified throughout the study to improve the potential benefits of the proposed control strategy. These include:

- The performance of the artificial neural network may benefit from further refinement of the structure of the network, and this requires further in-depth study.
- The refinement of the hydrodynamic torque estimation used in this study, in particular by considering the use of more advanced hydrodynamic models or machine learning tools.
- The optimisation of the PTO damping considering survivability criteria, by e.g. moving away from the damping coefficient leading to the maximum absorbed power in cases where the resulting PTO force reaches its capped value, to instead reduce the total bearing torque. In such cases, both the total PTO force and the distribution between PTOs could be varied.
- The extension of the study to consider extreme loads that are likely to be driven by extreme sea states and/or fault scenarios.
- Regarding the wave-by-wave damping control, more complex strategies (e.g. introducing a 'mass' and/or 'stiffness' term into (4)) could potentially lead to more significant increase in power capture, and could be investigated further.

APPENDIX

Percentage occurrences of each sea state were derived from a 10-year SWAN wave dataset (covering the period between January 1997 and December 2006). Fig. 13 to Fig. 19 summarise the occurrences for each direction.

H_s [m] / T_p [s]	7	9	11	13	15
0.75	0.2%	1.0%	0.4%	0.1%	0.0%
1.25	0.2%	1.1%	1.6%	0.6%	0.1%
1.75	0.0%	0.3%	1.8%	1.0%	0.3%
2.25	0.0%	0.1%	0.8%	1.2%	0.4%
2.75	0.0%	0.0%	0.2%	1.0%	0.3%
3.25	0.0%	0.0%	0.1%	0.5%	0.5%
3.75	0.0%	0.0%	0.0%	0.2%	0.4%
4.25	0.0%	0.0%	0.0%	0.0%	0.1%

Fig. 13. Wave occurrence matrix, 0° heading. Total = 14.4%, after scaling such that the total of all sea states considered = 100%

H_s [m] / T_p [s]	7	9	11	13	15
0.75	0.5%	1.6%	0.8%	0.2%	0.1%
1.25	0.3%	2.0%	2.6%	1.2%	0.4%
1.75	0.0%	0.5%	2.5%	1.9%	0.5%
2.25	0.0%	0.1%	1.3%	2.0%	0.7%
2.75	0.0%	0.0%	0.4%	1.4%	0.7%
3.25	0.0%	0.0%	0.1%	0.7%	0.6%
3.75	0.0%	0.0%	0.0%	0.2%	0.5%
4.25	0.0%	0.0%	0.0%	0.1%	0.3%

Fig. 14. Wave occurrence matrix, +/- 5° heading. Total = 24.3%, after scaling such that the total of all sea states considered = 100%

H_s [m] / T_p [s]	7	9	11	13	15
0.75	0.6%	1.6%	0.9%	0.2%	0.1%
1.25	0.4%	1.7%	2.1%	0.8%	0.2%
1.75	0.1%	0.6%	2.3%	1.6%	0.4%
2.25	0.0%	0.2%	0.9%	1.2%	0.4%
2.75	0.0%	0.1%	0.4%	0.8%	0.4%
3.25	0.0%	0.0%	0.2%	0.5%	0.3%
3.75	0.0%	0.0%	0.0%	0.2%	0.2%
4.25	0.0%	0.0%	0.0%	0.1%	0.1%

Fig. 15. Wave occurrence matrix, +/-10° heading. Total = 19.5%, after scaling such that the total of all sea states considered = 100%.

H_s [m] / T_p [s]	7	9	11	13	15
0.75	0.5%	1.2%	0.7%	0.2%	0.0%
1.25	0.6%	1.4%	1.6%	0.6%	0.1%
1.75	0.2%	0.9%	2.0%	0.9%	0.2%
2.25	0.0%	0.1%	1.0%	1.1%	0.3%
2.75	0.0%	0.1%	0.4%	0.8%	0.2%
3.25	0.0%	0.0%	0.1%	0.4%	0.3%
3.75	0.0%	0.0%	0.0%	0.2%	0.1%
4.25	0.0%	0.0%	0.0%	0.1%	0.1%

Fig. 16. Wave occurrence matrix, +/-15° heading. Total = 16.5%, after scaling such that the total of all sea states considered = 100%.

H_s [m] / T_p [s]	7	9	11	13	15
0.75	0.4%	0.8%	0.3%	0.1%	0.0%
1.25	0.9%	1.2%	1.0%	0.4%	0.0%
1.75	0.5%	1.0%	1.4%	0.5%	0.1%
2.25	0.1%	0.4%	0.9%	0.6%	0.1%
2.75	0.0%	0.1%	0.3%	0.4%	0.2%
3.25	0.0%	0.0%	0.1%	0.2%	0.1%
3.75	0.0%	0.0%	0.1%	0.1%	0.1%
4.25	0.0%	0.0%	0.0%	0.1%	0.0%

Fig. 17. Wave occurrence matrix, +/-20° heading. Total = 12.4%, after scaling such that the total of all sea states considered = 100%.

H_s [m] / T_p [s]	7	9	11	13	15
0.75	0.1%	0.1%	0.1%	0.0%	0.0%
1.25	1.1%	0.6%	0.2%	0.0%	0.0%
1.75	1.0%	0.9%	0.4%	0.1%	0.1%
2.25	0.3%	0.7%	0.3%	0.2%	0.0%
2.75	0.0%	0.2%	0.2%	0.1%	0.0%
3.25	0.0%	0.1%	0.1%	0.1%	0.0%
3.75	0.0%	0.0%	0.0%	0.0%	0.0%
4.25	0.0%	0.0%	0.0%	0.0%	0.0%

Fig. 18. Wave occurrence matrix, +/-25° heading. Total = 7.0%, after scaling such that the total of all sea states considered = 100%.

H_s [m] / T_p [s]	7	9	11	13	15
0.75	0.0%	0.1%	0.0%	0.0%	0.0%
1.25	0.8%	0.5%	0.1%	0.0%	0.0%
1.75	1.2%	0.8%	0.1%	0.0%	0.0%
2.25	0.2%	0.7%	0.2%	0.0%	0.0%
2.75	0.0%	0.4%	0.1%	0.1%	0.0%
3.25	0.0%	0.1%	0.1%	0.0%	0.0%
3.75	0.0%	0.0%	0.1%	0.0%	0.0%
4.25	0.0%	0.0%	0.0%	0.0%	0.0%

Fig. 19. Wave occurrence matrix, +/-30° heading. Total = 5.8%, after scaling such that the total of all sea states considered = 100%.

ACKNOWLEDGEMENT

This project has received funding from the European Union's Horizon 2020 research and innovation programme under grant agreement No 763959.

REFERENCES

[1] P. Laporte Weywada, J. Cruz, J. Scriven, M. Vuorinen and T. Maki, "Preliminary validation of a 1MW oscillating wave surge converter WEC-Sim model", *Proceedings of the EWTEC 2019*, Naples, Italy, 2019.

[2] N.R.R.C. Booij, R.C Ris, and L.H. Holthuijsen, "A third-◎generation wave model for coastal regions: 1. Model description and validation" *Journal of Geophysical Research: Oceans*, 104, 7649-7666, 1999.

[3] M.C. Deo and C.S. Naidu, "Real time wave forecasting using neural networks", *Ocean Engineering*, 26, 191-203, 1998.

[4] F. Fusco and J.V. Ringwood, "Short-term wave forecasting for real-time control of wave energy converters", *IEEE Transactions on Sustainable Energy*, 1, 99-106, 2010

[5] M.S. Roulston, J. Ellepola, J. von Hardenberg, and L.A. Smith, "Forecasting wave height probabilities with numerical weather prediction models", *Ocean Engineering*, 32, pp.1841-1863, 2005.

[6] G. Reikard and W.E. Rogers, "Forecasting ocean waves: Comparing a physics-based model with statistical models", *Coastal Engineering*, 58, 409-416, 2011.

[7] Fusco, F. and Ringwood, J.V., 2011. A study of the prediction requirements in real-time control of wave energy converters. IEEE Transactions on Sustainable Energy, 3(1), pp.176-184.

[8] N.K. Kumar, R. Savitha, A. Al Mamun, "Regional ocean wave height prediction using sequential learning neural networks" *Ocean Engineering*, 129, 605-612, 2017.

[9] V. Roeber, K.F. Cheung, and M.H Kobayashi, "Shock-capturing Boussinesq-type model for nearshore wave processes", *Coastal Engineering*, 57, 407-423, 2010.

[10] Y.-H. Yu, M. Lawson, K. Ruehl, and C. Michelen, "Development and demonstration of the WEC-Sim wave energy converter simulation tool", in *proceedings of the 2nd marine energy technology symposium*, METS 2014, Seattle, 2014.

[11] P.B. Garcia-Rosa, J.Ringwood, "On the sensitivity of optimal wave energy device geometry to the energy maximizing control system", Institute of Electrical and Electronics Engineers (IEEE) Transactions on sustainable energy, vol.7, no.1, 1 January 2016.

[12] K.Bubbar, B.Buckham, "On establishing an analytical power capture limit for self-reacting point absorber wave energy converters based on dynamic response", Applied Energy, Vol.228, 15 Octoer 2018, p.324-338.